Finite Element Evaluation of *J*-integral in 3D for Nuclear Grade Graphite Using COMSOL-Multiphysics

Awani Bhushan*[1], S.K. Panda[1], Sanjeev Kumar Singh[1], Debashis Khan[1]
[1]Indian Institute of Technology (BHU) Varanasi
*Corresponding author: Department of Mechanical Engineering, IIT (BHU) Varanasi, awanibhu@gmail.com

Abstract: It is well known that the computation of *J*-integral for 3D is a challenging task even for a unimodular case due to the presence of additional area integral term. The stress dependent elasticity formulation required for this study has been carried out using commercial finite element software COMSOL Multiphysics 4.4. Evaluation of *J*-integral in three dimensional bimodular stress field has been carried out for a cracked three point bend specimen. It has been observed that in contrast to unimodular models the degree of path independency is inferior in nature as the E_T/E_C ratio deviates from the value of unity. Also, the E_T/E_C ratio influences the value of the *J*-integral significantly. The severity of bimodular 3d crack progression behavior has been delineated with asymmetry of stress-distribution and distortion of neutral surface.

Keywords: 3D *J*-integral, bi-modular material, nuclear grade graphite, stress dependent elasticity,

1. Introduction

The development of dependable design and material characterization methods for the graphite structures used in the reactor are important to the NGNP (Next Generation Nuclear Power) Project because large amount of graphite (up to thousands of tons) would be required for the reactor core and because the individual graphite bricks that surround the nuclear fuel may experience significant loads. These graphite bricks has the potential for crack formation and even rupture in individual blocks. Therefore, failure theories and/or effective design strategies that can predict and mitigate failure from fracture are needed. An important characteristic of graphite is that its strength is stochastic means an individual specimen can show a large random fluctuation in strength from a population mean. Graphite can also have a nonlinear stress–strain response, and this behavior can be different in tension than in compression. Even though the analysis of materials exhibiting different tension/ compression characteristics was recognized by Saint-Venant in [1], however, the concept had not received much attention for a long time from research community. Later on, the concept of a bi-modular material was revisited by Timoshenko, while considering the flexural stress in such a material undergoing pure bending [2]. The effective modulus for stiffness of such a beam in pure bending was given by Marin [3]. The bimodulus concept was extended to two-dimensional materials by Ambartsumyan [4-6]. Within the last few decades several attempts have been made to establish constitutive relationships for such materials and develop analytical and numerical solutions for the bending and shear deformation of bimodular beams [7-13]. However, very few of these devote to the criticality of bimodularity along the 3-D crack front due to its inherent complexity of singularity in the third direction along with stress dependent elasticity modulus. There is no secret of the fact that materials like graphite, ceramic and such other synthetic material used in high risk components have different modulus in tension and compression depending on the overall state of stress under various loading conditions. Therefore design models are heavily dependent on unrealistic factor of safety parameter, which sometimes make even the feasibility of the system redundant in comparison to other standard dimensions for similar parts. This has added to the uncertainty and low level of confidence among research community while designing nuclear reactor components made of graphite material. Therefore the authors feel, it will be a worthwhile exercise to formulate a research problem with an objective to tackle three dimensional crack field in a bimodular material aiming at minimizing catastrophic failures of graphite clad components. For assessing the fracture behavior of such materials, characterization of *J*-integral is very much involved and the present study devote to quantify it for evaluating criticality of bimodularity for studying three dimensional crack progression behaviors. In the present study, COMSOL Multiphysics 4.4, finite element analysis software has been used to evaluate the deformation, stress, and the *J*-integral in 3D for a bi-modular three point bend cracked specimen as shown in Fig. 1. The properties of nuclear grade graphite material incorporated in this study has been referred from graphite design hand book [14]. The evaluation of *J*-integral for 3D is a tedious task even for a unimodular case due to the presence of additional area integral term. Due to the availability of stress dependent elasticity formulation required for the constitutive equation in bimodularity in COMSOL Multiphysics 4.4, the authors are motivated here for the studies of *J*-integral in 3D for nuclear grade graphite. The analysis is carried out to explore the variation of the *J*-integral with respect to the E_T/E_C ratio for a number of different integration contours around the crack tip. Also the combined effect of loading and bimodularity has been studied for same specimen.

2. Problem Description and Finite Element Model

2.1 Specimen Geometry

A cracked three point bend specimen has been analyzed under distributed point load along the width Z shown in Figure 1 and 2. The specimen geometry is cracked throughout the width Z. The edge crack length is 5 mm. The length of specimen is 20 mm and the breadth (Z) and thickness (t) are equal to 25 mm. The finite element simulation was performed for nuclear grade graphite (grade 2020). The Young's Modulus of elasticity for this graphite in tension is found to be 7.14757 GPa whereas in compression is 3.89549 GPa by analyzing stress-strain curve [14]. The simulation for a range of E_T/E_C ratio and also for a range of applied point load have been done, in COMSOL Multiphysics 4.4.

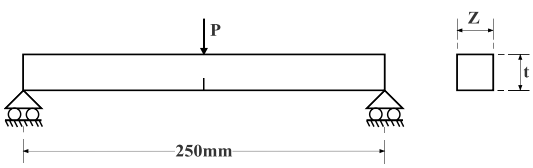

Figure 1: Cracked three point bend specimen

2.2 Finite Element Model

The complex model built using COMSOL for desired mesh distribution control as well as contour formation for calculating *J*-integral has been shown in Figure 2. The mesh distribution in whole geometry as well as around the crack tip has been shown in Figure 3 and 4 respectively. There are 14520 hexahedral elements present in the numerical analysis.

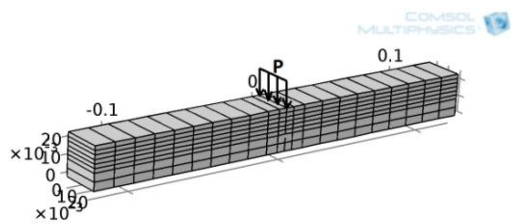

Figure 2: Finite Element model built for controlling symmetrical mesh to define contour to evaluate the *J*-integral for cracked three point bend specimen

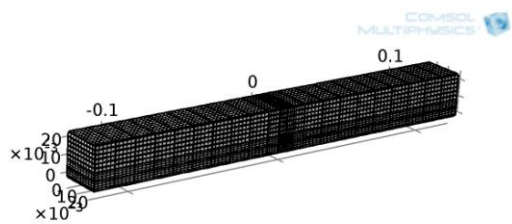

Figure 3: Finite Element model mesh for specimen.

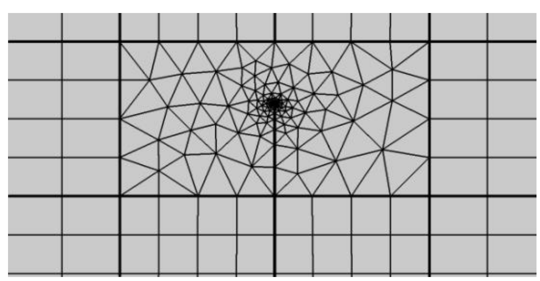

Figure 4: Finite Element model mesh around the crack tip.

2.3 Bimodular formulation

Some natural and man-made materials which exhibit different elastic moduli in tension and compression are known as bi-modulus materials. When we perform the flexural testing the effect of bi-modularity really works because the top half portion of the specimen posses compression and the other half of the portion posses tension. The implementation of this property in finite element model is quite challenging task. The model formulation has been done using stress dependent elasticity, and the following steps are availing the bi-modular formulation:

1. 1st iteration is the linear model formation where taking some arbitrary value of Young's Modulus of elasticity. That means the model is solved for unimodular condition, then after we found the stress distribution at each node.

2. Sense the stress value at each node.

3. Evaluate the value of variable p at each node. where p is negative hydrostatic stress.
$$p = -\left(\frac{\sigma_{xx} + \sigma_{yy} + \sigma_{zz}}{3}\right) \tag{1}$$

4. For next iteration we have to put the E_T (Young's Modulus of elasticity in tension) and E_C (Young's Modulus of elasticity in compression) according to following criteria, where Young's Modulus of elasticity is defined by a step function.

5. The modulus of elasticity of material is define a step function, which sense the value of p
$$E(p) = \begin{Bmatrix} E_T\, where, -p \\ E_C\, where, +p \end{Bmatrix} \tag{2}$$

6. Putting the E_T and E_C value at the nodes by finding where the value is -p and +p respectively and again solve the problem.

7. The iteration continues until the error became less than tolerance limit.

8. So, the duration of solving the problem is greatly increased by mesh refinement and reducing the tolerance limit.

9. So, finding appropriate solution in 3D is quite a difficult task because the solution time is too long.

3. Evaluation of *J*-integral for 3D

The *J* integral is an alternative way to compute the point-wise value *J*. It is defined as the combination of a path integral and an area integral [15-18]. In order to characterize 3D elastic crack problems, it is customary to compute the point-wise value of *J* along a 3D crack front. This point-wise value is usually denoted as *J(s)*, where s is a parametric coordinate that defines the crack front position, as shown in Figure 5.

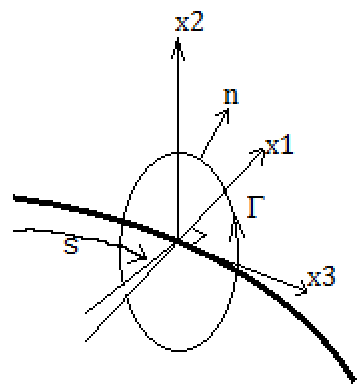

Figure 5: local cartesian coordinate system at a point s of the crack front.

A local Cartesian coordinate system is conventionally defined as follows: the x2 axis is perpendicular to the plane tangential to the crack at s and the x1 and x3 axes lie in that tangential plane, being normal and tangent to the crack front, respectively. Many works regarding the computation of *J* can be found in the literature and we do not intend to make a thorough review of them [19]. For the sake of completeness, we introduce below the definitions and nomenclature that will be used in the rest of the study. Carpenter, Read and Dodds [16, 20] had given the expression for the *J* integral of local crack extension for 3D geometries and the expression is given as:

$$J(s) = JC_1(s) + JC_2(s) + JC_3(s) + JA_1(s) + JA_2(s) + JA_3(s) \tag{3}$$

where $J_{Ci}(s)$ is the line integral evaluated over a contour that lies in the principal normal plane of the crack front at "s" and that encloses the crack tip. $J_{Ai}(s)$ denotes an integral evaluated over the area enclosed by the contour. Then each and every integral is defined by:

$$J_{C1}(s) = \oint_{\Gamma} W^e n_1 d\tau \tag{4}$$

$$J_{C2}(s) = \oint_{\Gamma} W^p n_1 d\tau \tag{5}$$

$$J_{C3}(s) = -\oint_{\Gamma} u_{i,1} T_i d\tau \qquad (i=1,2,3) \tag{6}$$

$$J_{A1}(s) = -\oint_{A} W^p_{,1} dA \tag{7}$$

$$J_{A2}(s) = \oint_{A} \left(\sigma_{ij} \varepsilon^p_{ij,1}\right) dA \qquad (i=1,2,3) \tag{8}$$

$$J_{A3}(s) = -\oint_{A} (\sigma_{i3} u_{i,1})_{,3} dA \qquad (i=1,2,3) \tag{9}$$

where,

$$W = \int_0^{\varepsilon} \sigma_{ij} d\varepsilon_{ij} \,; \quad W^e = \frac{1}{2}\sigma_{ij}\varepsilon_{ij} \,;$$

$$W^p = W - W^e$$

Here we assumed that the material is linear elastic, the $J_{C2}(s)$, $J_{A1}(s)$, and $J_{A2}(s)$ integrals are vanished. For an elastic material in plane stress and plane strain the term $J_{A3}(s)$ also vanishes ,i.e, the case of 2D but in 3D for an elastic material $J(s)$ consists of all the three terms as $J_{C1}(s)$, $J_{C3}(s)$ and $J_{A3}(s)$.

$$J(s) = J_{C1}(s) + J_{C3}(s) + J_{A3}(s) \tag{10}$$

$$J(s) = \oint_{\Gamma} W^e n_1 d\tau - \oint_{\Gamma} u_{i,1} T_i d\tau - \oint_{A} (\sigma_{i3} u_{i,1})_{,3} dA \qquad (i=1,2,3) \tag{11}$$

$$J(s) = \oint_{\Gamma} \left(W^e n_1 - u_{i,1} T\right) d\tau - \oint_{A} (\sigma_{i3} u_{i,1})_{,3} dA \qquad (i=1,2,3) \tag{12}$$

The $J(s)$ contains two integrals: the first is a path integral and the second is an area integral. Both the path Γ and the area enclosed by the path Γ lay in x1-x2 plane which is perpendicular to the crack front. In computing $J(s)$ the derivatives of stresses, strains and displacements are required, and when based on numerical approximations their values at the vicinity of a singular point is poor. Therefore the computation of the area integral is a difficult task with reasonable accuracy. It is clear that $J_A \to 0$ in the two-dimensional conditions of plane stress and plane strain. In a general 3D crack problem, it can be proved that $J(s)$ is equivalent to the Rice's J-integral [21], because J_A vanishes when Γ→0 since the area J_A reduces to 0 and the integrand in J_A is non-singular (Dodds and Read, 1990)[22].

3.1 Contour Formation

The evaluation of *J*-integral for 10 contours is used in which 8 contours are shown in the figure and remaining two contours are overlapping between contours. The line integral is evaluated for the following contours (shown in Figure 6) whereas area integral is evaluated for area made by contour along crack front.

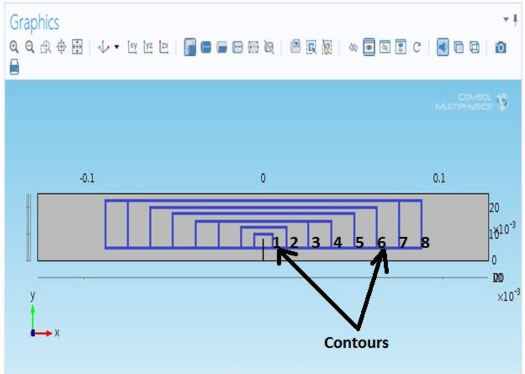

Figure 6: Contours for evaluating *J*-integral value

4. Results and Discussion

The figure 7 and 8 describe that the stress distribution around the crack tip is quite high with respect to other part of the beam (for the applied point load 500N).

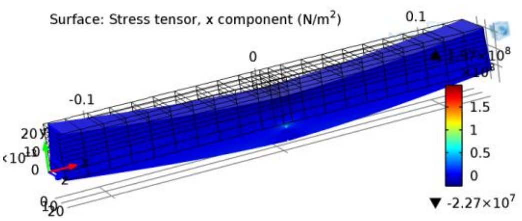

Figure 7:Normal stress distribution in X-direction

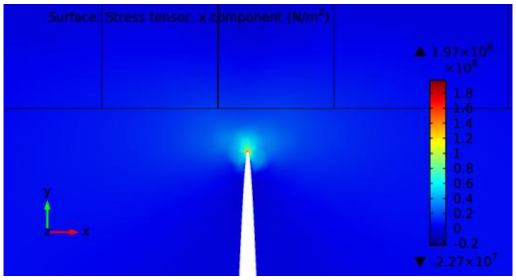

Figure 8: Normal stress distribution in X-direction around the crack tip.

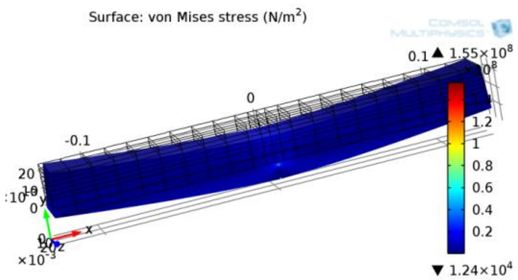

Figure 9: Von-Mises stress distribution for three point bend specimen

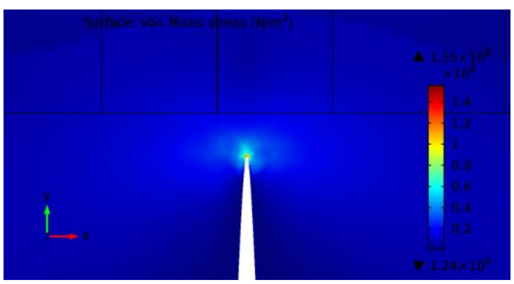

Figure 10: Von-Mises stress distribution around the crack tip for three point bend specimen

Similar sort of distribution pattern have been found for Von-Mises stress distribution shown in figure 9 for whole geometry whereas figure 10 represents the distribution around the crack tip.

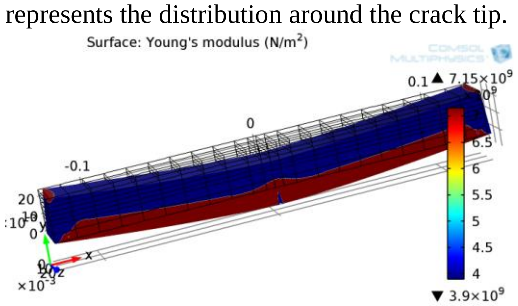

Figure 11: Young's Modulus plot for the three point end specimen

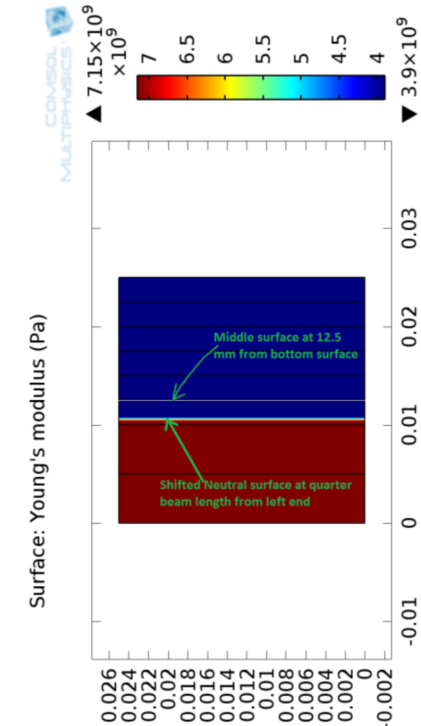

Figure 12: Young's Modulus plot for a cross-section at quarter of the beam and are showing the shift of neutral surface.

The young' modulus of elasticity plot for the bimodular beam in deflected condition has been shown in Figure 11. It is well reflected the region of tension and compression. Whereas Figure 12 represents that Young's Modulus plot for a cross-section surface at quarter of the beam from left end and are showing the shift of neutral surface from the middle.

Figure 12 shows the variation between normalized *J* integral with different E_T/E_C ratio at all contours. Here, the values of the *J*-integral is normalized by the average *J*-integral value where E_T/E_C ratio is unity. In this graph the path independent behavior of the *J*-integral is well preserved. It is observed here that for lower E_T/E_C ratio variations in the value of *J*-integral is more as compared to higher E_T/E_C ratio. The degree of path independency is going to be slightly inferior in nature as the E_T/E_C ratio deviates from the value of unity. The value of *J*-

integral is significantly increases by increasing E_T/E_C ratio.

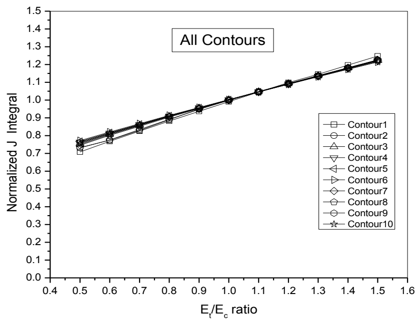

Figure 12: Normalized *J*-integral vs. E_T/E_C ratio at all contours

Figure 13 demonstrates the variations of total *J*-integral with different loads at different E_T/E_C ratio. Here, the values of total *J*-integral is first normalized by the maximum value then plotted against different loads. It is observed that the value of *J*-integral is varying from 0 to 1.2 and there is the significant difference in the values of *J*-integral for different E_T/E_C ratio. It is also observed here that as the load increases, *J*-integral values also increases significantly.

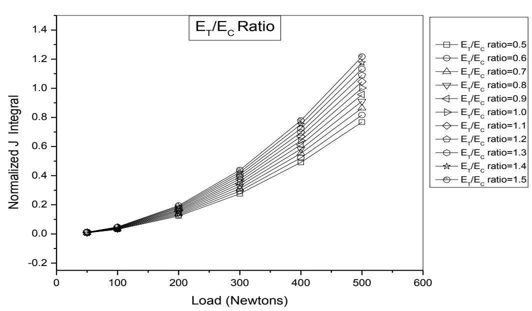

Figure 13: Normalized *J* vs. different loading at different E_T/E_C ratio.

5. Conclusions

It is reflected that the path independency is well preserved here. The degree of path independency is going to be slightly inferior in nature as the E_T/E_C ratio deviates from the value of unity. Also it is observed that the E_T/E_C ratio influences the value of the *J*-integral significantly. For very low load level, it is apparent that all the *J*-values merge into a single parabolic curve for different E_T/E_C ratio, however with increase in load level, strong divergence in the *J*-value occur for different E_T/E_C ratio. Therefore, it is concluded that the effect of the bi-modularity on the computation of *J*-integral values cannot be neglected.

6. References

1. Saint-Venant B., "Notes to Navier's Resume des lecons dela resistance des corps solids," 3rd Ed., Paris, 175 (1864).
2. Timoshenko S., "Strength of materials, Part2." Advanced Theory and Problems, 2nd Ed., Van Nostrand, Princeton, N.J., 362–369 (1941).
3. Marin J., "Mechanical behavior of engineering materials," Prentice- Hall, Englewood Cliffs, N.J., 86–88 (1962).
4. Ambartsumyan S.A. "The axisymmetric problem of circular cylindrical shell made of materials with different stiffness in tension and compression." Izvestia Akademiya Nauk SSSR. Meckanika,. (4), 77-85; English Translation (1967), NTIS Report FTD-HT-23-1055-67, Nat. Tech. Info. Service, Springfield, Va (1965),.
5. Ambartsumyan S.A., "Equations of the plane problem of the multimodulus theory of elasticity," Izvestiya Akademii Nauk Armanskoi SSR, Mekhanika, 19(2), 3-19. Translation available from the Aerospace Corp., El Segundo, Calif, as LRG-67-T-14 (1966).
6. Ambartsumyan, S.A., "Basic equations and relations in the theory of elasticity of anisotropic bodies with different moduli in tension and compression." Inzhenemyi Zhurnal, Mekhanika Tverdogo Tela, 3, 51-61. Translation available from the Aerospace Corp., El Segundo, Calif, as LRG-70-T-1(1969).
7. Bert, C.W. "Models for fibrous composites with different properties in tension and compression," Eng. Mat. and Tech. Trans., ASME, 99H, Oct., 344- 349(1977),.
8. Bert, C.W., "Recent advances in mathematical modeling of the mechanics of bimodulus, fiber-reinforced materials," Proc. 15th Annual Meeting, Society of Eng. Science, Gainesville, Fla., Dec, 101-106, (1978).
9. Green, A.E., and Mkrtichian, J.Z., "Elastic solids with different moduli in tension and compression," J. Elasticity, 7(4), 369-386, (1977).

10. Isabekian, N.G., Khachatryan, A.A., "On the multimodulus theory of elasticity of anisotropic bodies in plane stress state," Ivestiya Akademii Nauk Armianskoi SSR, Mekhanika, 22(5), 25-34. Translation available from R. M. Jones, (1969).
11. Jones, R.M., "Buckling of stiffened multilayered circular cylindrical shells with different orthotropic moduli in tension and compression," AIAA Journal, 9(5), 917-923, (1971).
12. Jones, R.M., "Stress strain relations for materials with different moduli in tension and compression," AIAA Journal, 15(1), 16-23, (1977).
13. Iwase T., Hirashima K., "High-accuracy analysis of beams of bimodulus materials," Journal of Engineering Mechanics, (126)149-156, (2000).
14. General Atomics "Graphite design handbook", , DOE-HTGR-88111, (1988).
15. Blackburn, W.S., "Path independent integrals to predict onset of crac instability in an elastic plastic material", International Journal of Fracture Mechanics, vol. 8, pp. 343–346, (1972).
16. Dodds, R.H., Jr., "Finite Element Evaluation Of J Parameters In 3D", International Journal of Fracture, vol. 33, pp. R7-R15, (1987).
17. Chiarelli, M. and Frediani, A., "A computation of the 3-dimensional J-integral for elastic-materials with a view to applications in fracture-mechanics", Engineering Fracture Mechanics, vol. 44(5), pp. 763–788, (1993).
18. Huber, O., Nickel, J. and Kuhn, G., "On the decomposition of the J-integral for 3D crack problems", International Journal of Fracture, vol. 64(4), pp. 339–348, (1993).
19. Omer, N., and Yosibash, Z., "On the path independency of the point-wise *J* integral in three-dimensions", International Journal of Fracture vol. 136, pp. 1–36, (2005).
20. Carpenter, W.C., Read, D.T., "Comments On The Evaluation of the 3D Integral", International Journal of Fracture, vol. 26, pp. R71 - R74, (1984).
21. Rice, J.R., "A path independent integral and the approximate analysis of strain concentration by notches and cracks." Trans. ASME, J. Appl. Mech., vol. 35, pp. 379-386, (1968).
22. Dodds,R. H. Jr. and Read D. T., "Experimental and numerical studies of the J-integral for a surface flaw.", International Journal of Fracture 43: 47-67, (1990).

7. Acknowledgements

The authors wish to gratefully acknowledge the financial support for this research provided by BRNS under Grant No. 2011/36/62-BRNS with Indian Institute of Technology (Banaras Hindu University).